SSRG International Journal of Mechanical Engineering
ISSN: 2348-8360/ https://doi.org/10.14445/23488360/IJME-V11I12P101

Volume 11 Issue 12, 1-21, December 2024

Original Article

Enhancing Heat Transfer in Heating of PET Bottles for Carbonated Beverages

Gagan Malik[1], Arvind kumar Mahalle[2], Rohit P. Sarode[3], Shreya Malik[4]

[1,2,3]*Department of Mechanical Engineering, G. H. Raisoni University, Amravati, Maharashtra, India.*
[4]*Department of Computer Science and Engineering, Indian Institute of Information Technology, Guwahati, India.*

[1]*Corresponding Author : gaganimalik@gmail.com*

Received: 05 October 2024 Revised: 15 November 2024 Accepted: 02 December 2024 Published: 27 December 2024

Abstract *- This study investigates the enhancement of Heat Transfer (HT) during the heating process of PET-used PET (Polyethylene Terephthalate) bottles used for carbonated beverages, aiming to improve the efficiency and consistency of temperature distribution. This research provides a theoretical analysis to decide how the arrangement of bottles affects the quantity of energy stored in a solar heating system. The Thermal Energy Storage (TES) performance of commonly used PET bottles, ranging in size from 0.25,0.33,0.4,0.5,0.6,0.75,1.25, 2,2.25 x $10^{-3}m^3$ and filled with chilled beverages at 280 kelvin and capped, has been examined while passing through warming Tunnel and hot air passed over the PET bottles with different velocities. The overall capacity of the energy transferred is inline arranged 924-2079,648-1499,358-819 x $10^{-3}m^3$ with bottle Gap 0.25d,0.5d,1d respectively, and Staggered 892-1935,621-1377,338-729 x $10^{-3}m^3$ with bottle Gap 0.25d,0.5d,1d respectively, A theoretical study has been conducted on the impact of intake velocity, intake temperature, bottle capacity, along with bottle layout on the quantity of energy. This study is particularly valuable for enhancing HT during the heating of PET bottles for carbonated beverages, as it offers insights into optimizing bottle arrangements and airflow conditions to improve thermal efficiency. By optimizing these factors, the heating process can be made faster and more energy-efficient, ensuring better quality and consistency in beverage production. Upon concluding this research, it has been shown that employing chilled beverage-filled PET bottles in the sensible thermal energy system is a practical, uncomplicated, and cost-effective method for transferring solar energy. Furthermore, due to the energy storage capabilities of PET bottles, there is no need for a heat exchanger during the charging operations. The working fluid, air, directly flows over PET bottles during the charging phases. It has been noted that reducing the diameter (volume) of the bottle resulted in an increase in the quantity of thermal energy.*

Keywords *- Heat transfer (HT), PET bottle, solar energy, Bottle arrangement, TES.*

1. Introduction

The growing focus on renewable energy applications, reducing energy consumption, and optimizing energy management has become critical to addressing environmental issues as well as mitigating the effects of the global energy crisis. With the increasing energy demands in both building and industrial sectors globally, there is a need for innovative methods to enhance the thermal efficiency of cooling and heating systems. The market is searching for advanced materials, technologies, and systems to reduce reliance on fossil fuels, harness renewable energy sources, promote greener energy usage, and sustainably and cost-effectively improve indoor thermal comfort. Aside from heating, one of the beverages' most significant energy requirements is removing heat before stacking finished goods. In this context, using PCMs for heat transfer is essential to achieving energy savings and balancing peak demand with energy production. However, the current application of PCMs presents challenges, particularly in terms of cost-effectiveness and implementation strategies. This is highlighted by the ongoing research and practical evaluations of these materials. [1][2]. High thermal energy densities may be stored in a constrained temperature range using effective technologies like PCMs and TES.

Early mass-produced PET had limited performance because of the constraints of chemical and mechanical technologies, which is much lower than the current standards. Consequently, the bottom of the bottle is intentionally shaped like a hemisphere to distribute the pressure evenly as much as possible. It also has a removable base component to ensure the bottle remains upright [3]. Nevertheless, advancements in science and technology have led to the replacement of PET bottles with hemispherical bottoms. These have been substituted with more customized and varied shapes, including bottle bottoms with radial grooves, concave pentagonal petal bottoms, and the claw-petal bottom structure pioneered by the Coca-Cola Company [4][5]. These single-

step blow moulding designs save manufacturing costs, streamline production processes, and provide more convenience and sustainability. However, as compared to the hemispherical base, it is more prone to cracking due to the mechanical qualities resulting from microscopic crystallinity and molecular orientation [6][7][8], as well as the more noticeable stress concentration when seen on a larger scale [9][10][11].

PET bottles, widely used for packaging carbonated beverages, undergo a preheating stage to prepare them for blow moulding. This process shapes the bottles by heating them to a specific temperature. Efficient HT during this stage is crucial to ensure uniform heating, prevent material degradation, and achieve the desired mechanical properties of the bottles. The research focuses on innovative techniques and methodologies to enhance the HT rate, such as optimizing the heating environment, utilizing advanced thermal management systems, and exploring novel materials and surface coatings. Improved HT can lead to faster production cycles, reduced energy consumption, and lower operational costs while ensuring the structural integrity and safety of the bottles under high-pressure carbonation conditions. This study also examines the impact of enhanced HT on the overall sustainability of the manufacturing process, contributing to more eco-friendly production practices by minimizing waste and energy usage.

1.1. Problem Statement

The increasing demand for energy-efficient systems in beverage production, particularly in the preheating of PET bottles used for carbonated beverages, has led to a need for improved heat transfer (HT) methods. Current preheating processes are inefficient, leading to longer production cycles, higher energy consumption, and potential material degradation. Although various studies have explored heat transfer enhancement through thermal management, the arrangement and different sizes of PET bottles and the influence of air velocity and temperature have not been thoroughly investigated. This research attempts to bridge this gap by examining how the arrangement of PET bottles, their size, and airflow conditions affect thermal efficiency, specifically in solar heating systems used for carbonated beverage PET bottle heating after chilled filling. It is essential to develop strategies that optimize these factors to improve the overall efficiency and sustainability of the heating process.

1.2. Research Gap

While numerous studies have focused on optimizing individual parameters such as air velocity, temperature, or bottle size in heating systems, there remains a lack of comprehensive studies that systematically analyze the combined effect of these variables in the context of PET bottles for carbonated beverages. Specifically, the impact of bottle arrangement (inline vs. staggered configurations), bottle size variation, and airflow velocity on heat transfer efficiency during the heating phase has not been adequately explored. Additionally, there is a gap in the exploration of using solar heating systems for carbonated beverage-filled PET bottle heating and how such systems can be optimized along with Thermal Energy Storage (TES) performance without relying on traditional heating systems. This research addresses these gaps by providing a thorough theoretical and experimental analysis of the factors influencing HT, including TES performance in carbonated beverage chilled-filled PET bottle heating.

1.3. Novelty of Work

This study presents a novel approach by integrating solar heating systems with Carbonated beverage chilled-filled PET bottles as thermal energy storage units, eliminating the need for conventional heating systems. It innovatively explores the effect of different bottle arrangements (inline vs. staggered) on thermal efficiency alongside variations in bottle size and air velocity. The research also provides valuable insights into optimizing the use of PET bottles, commonly used for carbonated beverages, as an effective medium for solar-based heat transfer, which has not been extensively studied in the context of beverage packaging. Additionally, by focusing on a broader range of factors affecting HT efficiency and energy storage capabilities, this research aids in creating a more environmentally friendly and energy-efficient heating process for the beverage industry. The findings can significantly enhance the design and operational strategies of thermal systems in beverage packaging, promoting environmentally friendly practices and reducing operational costs.

2. Literature of Review

The literature assessment on the impact of bottle layout on TES in solar heating systems, you might include further research and investigate similar topics in the following domains:

2.1. TES Systems: A Broader Context

- Din and Rosen (2011) provide an in-depth analysis of TES systems, classifying them into sensible, latent, and thermochemical storage [12]. Their work is essential to understanding the comparative strengths and weaknesses of every TES method, especially the role of sensible heat storage in solar applications.
- Zhang et al. (2016) reviewed the latest developments in TES technologies, focusing strongly on implementing TES in renewable energy systems [13]. They highlight key challenges in material selection and energy storage efficiency that could be useful when analysing the potential of water-filled PET bottles.
- Abhat (1983) is a classic study on TES materials and technologies, providing foundational knowledge on LHS and SHS. LHS in the 273-393K range is useful for space heating, domestic hot water, and solar cooling applications. Efficient storage systems rely on both heat-

of-fusion materials and heat exchangers. This review covers materials such as paraffins, fatty acids, and inorganic salt hydrates. Inorganic salts offer higher heat storage capacity but face issues like supercooling and decomposition. Understanding melting, freezing behaviour, thermal cycling, and material compatibility is crucial for long-term storage performance. Salt hydrates in sealed containers and metallic surfaces help reduce supercooling and improve reliability [14]. This paper can serve as a basis for understanding the evolution of TES systems and materials, which would contextualize more recent studies on water-filled PET bottles.

2.2. Recent Advancements in TES Technologies

- Stadler et al. (2019) discuss the integration of TES in solar energy systems, focusing on using water and other PCMs. They analyse the role of TES in enhancing energy efficiency by managing the intermittency of RESs, particularly solar [15].

- Kalaiselvam and Parameshwaran (2016) provide a comprehensive review of TES materials, focusing on new developments in latent and sensible heat storage. They highlight the emerging role of novel materials and hybrid systems for TES, which could offer comparative insights when assessing PET bottles [16].

- Gong et al. (2020) the paper proposes a model that uses an analogous thermal resistance for residential structures with HVAC systems derived from extensive electric power measurements during summer days. The model, based on a fully instrumented house typical of regional communities, is useful for VPP and DRS. An aggregation technique is also presented, applying a realistic distribution of HVAC loads, demonstrated through a study of 10,000 homes. The results show that by utilizing VPP controls and adjusting indoor temperatures, peak power demand during critical hours can be reduced by 20% and daily energy use by 4% [17]. Represented a case study on TES systems using a combination of water and low-cost recycled materials for community-level solar heating applications. This could provide valuable comparative data to the Dogan Erdemir et al. (2022) study, showing how PET bottles can be utilized in scalable, community-based solutions [18].

- Rucevskis et al. (2019) conducted practical case studies on TES systems in residential buildings using water-based storage mediums. This work evaluated an active PCM-based TES system using cold water through capillary pipes for thermal storage control. Simulations showed the active system reduced indoor temperatures by 279.9K, outperforming a passive system with poor PCM solidification at night. The standalone PCM units can be easily integrated into buildings, and results will guide prototype testing [19]. Their research could further emphasize the practicality of using PET bottles for small to medium-scale solar heating systems in various building types.

2.3. TES using Plastic Bottles

- Erdemir et al. (2019) this study examines the impact of bottle arrangements on sensible TES using water-filled PET bottles in a 1500 $x\ 10^{-3}\ m^3$ unit. Different bottle volumes (0.5, 1.5, and 5 $x\ 10^{-3}\ m^3$) and operating conditions like inlet temperature and velocity were analysed. PET bottles are affordable, recyclable, and suitable for low-temperature TES. Lower-volume bottles provide more stored heat, and no heat exchangers are needed. The study showed no discernible difference between staggered and inline configurations at higher Reynolds numbers. The highest stored energy (8.5 MW) was achieved with specific SN and SP values in the inline arrangement, confirming PET bottles as a cost-effective, ready-to-use solution for TES [20]. The study also explores the potential of recycled plastic bottles in thermal storage systems, offering new environmental perspectives. They emphasize the sustainability of using recyclable materials like PET bottles for heat storage and energy conservation. Their work adds an environmental and economic angle.

- Qin et al. (2022) PCMs are vital in storing and recovering waste heat, with container geometry playing a key role in their melting and HS performance. This study simulates PCM melting in containers with the same cross-sectional area but different shapes: rectangular, concave, and protruding sidewalls. Geometry impacts contact with hot airflow and natural convection during melting. The 3D transient modelling shows that stronger convection currents accelerate PCM melting [21]. The study conducted experimental studies using recycled plastic bottles in TES systems of different shapes and sizes. They observed how bottle arrangement and orientation affect energy retention, offering insights into how varied geometries, such as square versus cylindrical bottles, might influence system performance.

- Ahmed et al. (2023) this study improves pyramid solar stills by using PCM-encapsulated cylindrical fins of different heights. It shows that fins enhance performance, with 40 mm fins providing the best efficiency. Adding PCM further boosts efficiency and water productivity while reducing production costs compared to conventional stills [22]. The study evaluated the use of PET bottles as HS containers in passive solar energy systems. Their study explores different configurations, bottle sizes, and materials to optimize thermal performance in small to medium-scale TES units.

- Erdemir et al. (2018) this study investigates a solar heating system's thermodynamic performance using 5,120 water-filled 1.5 $x\ 10^{-3}\ m^3$ PET bottles for TES. The system was tested in October and November, with exergy and energy efficiencies of 51.89% and 79.85% in October

and 46.26% and 69.95% in November, respectively. Higher temperatures in October led to less heat loss and better performance. Efficiencies were higher during the charging period due to lower heat loss compared to the discharging period [23]. System efficiency can be improved by adjusting bottle arrangement volumes or using alternative storage materials. The study confirms PET bottles are an effective and low-cost energy storage solution.

- Ceja Soto et al. (2019**)** explored using waste PET bottles as TES units in low-cost solar water heating systems. This work focused on developing a sustainability measurement for housing, creating a PET-based prototype for walls and roofs, and evaluating its temperature and humidity. The prototype scored 67.74% on the sustainability scale, showing good insulation with stable internal temperatures lower than outside. Internal humidity ranged from 15% to 55%, while external humidity varied widely. Simulations indicated potential thermal performance, though factors like solar radiation were not included. Overall, the prototype demonstrated promising thermal stability and insulation properties [24]. Their study included a lifecycle assessment, highlighting the environmental benefits of recycling PET bottles for TES systems. This paper could offer insights into the sustainability aspects of PET usage.
- Reddy et al. (2018) TES is vital for balancing energy supply and demand, particularly with intermittent renewable sources. PCM-based storage offers significant potential for meeting large-scale energy needs. The functional principles, thermophysical characteristics, and other features of the many PCMs employed in TES systems are reviewed in this work. It discusses long-term stability, interactions with storage containers, and techniques to enhance HT and thermal conductivity. The paper also presents schematics of tested systems, results from prototype setups for thermal load management, and energy with exergy analyses of various storage systems [25]. This study provided experimental data on the energy storage capacity of PET bottles in TES systems. They compared cylindrical and spherical bottles, highlighting that the cylindrical shape showed better energy retention because of its large surface area-to-volume ratio. Their work can further support the findings from Ismail and Henriquez (2001) [26].

2.4. Thermal Stratification and HT in TES Systems

- Sifnaios et al. (2022) examined the effects of thermal stratification on water-based TES systems. Stratification in four storage settings was examined in this study: entirely mixed, fully stratified, and two realistic examples. It looked at four stratification indicators: MIX number, stratification coefficient, exergy efficiency, and overall exergy efficiency. While total exergy efficiency was beneficial, the other indicators had major downsides, making the results difficult to interpret. The study recommends using overall exergy efficiency along with internal exergy destruction to evaluate stratification in TES. This approach provides a thermodynamic basis for assessing stratification performance without relying on idealized storage simulations. Future work will explore applying these methods to real-life storage systems, highlighting their potential for comparing stratification across various applications [27]. This study discusses how maintaining thermal layers in storage tanks can improve system efficiency. This research can inform optimal storage arrangements since PET bottles are used as storage units in water-based TES.
- Erdemir et al. (2019**)** examined HT and stratification in cylindrical water containers for TES. They studied both inline and staggered arrangements, offering useful comparisons to findings on PET bottle configurations [20].
- Selimefendigil et al. (2021) This study assesses the performance of a PCM-filled vertical cylinder under surface corrugation and binary nanoparticles in the HT fluid, using numerical simulations with varying Reynolds numbers and corrugation parameters. Results show that higher Reynolds numbers and solid volume fractions significantly enhance thermal transport and reduce charging time, with a 57% reduction in charging time at the highest Reynolds number. At the same time, corrugation parameters negatively affect the process [28]. This study presented a numerical analysis of HT in spherical and cylindrical capsules for TES applications. This study provides a quantitative basis for understanding the HT mechanisms in PET bottle-based TES systems, especially when comparing cylindrical versus spherical shapes.

2.5. Bottle Volume and Arrangement Optimization

- Erdemir et al. (2019) analysed the role of container geometry and size on TES efficiency in large-scale solar power plants. This study includes a section on optimizing the volume of TES units, which directly applies to understanding how different bottle sizes (0.5, 1.5 and 5 $x\ 10^{-3}\ m^3$) perform in solar heating systems [20].
- Sedeh and Khodadadi (2013) study numerically and experimentally investigates the effective thermal conductivity of graphite foam infiltrated with PCM, demonstrating significant improvements over PCM alone. A three-dimensional model of the graphite structure was used for simulations. At the same time, experiments involved measuring temperature changes in infiltrated samples under fixed heat flux, confirming that natural convection within the pores is negligible and aligning with reported results on graphite foam. They studied the effects of container spacing and arrangement on HT in TES systems [29]. Their findings indicate that smaller bottles with greater surface area-to-volume ratios store more thermal energy, which aligns with Erdemir's

(2019) [20] conclusions about the benefits of smaller PET bottles.

2.6. Influence of Intake Temperature and Flow Velocity on TES Performance

- Zhang et al. (2023) analyse the impact of varying inlet temperatures on the performance of LHTESS through numerical simulations. The unsteady intake temperature of the HTF significantly outperforms the corresponding steady intake temperature at peak performance levels of the system. The thermal performance evaluation coefficient is higher for unsteady inlet temperatures compared to steady inlet temperatures. The parameters related to thermal performance [30].

- Erdemir et al. (2019) conducted a detailed experimental analysis of intake velocity and intake temperature on the thermal performance of sensible TES systems, which consist of water-filled PET bottles energy storage capacity of water-based TES systems. Their findings on how higher inlet temperatures can significantly increase thermal energy retention can be useful when optimizing PET bottle-based systems. As the inlet velocity increases, parameters such as Reynold number, energy stored, Nusselt number Nu, and HT coefficient also increase due to the enhanced turbulence in the storage unit, leading to a rise in stored energy. The effect of intake temperature on stored energy (Q stored), where higher inlet temperatures result in increased energy storage due to a greater temperature difference between the bottle surface and bulk temperature [20]. However, the rate of increase in stored energy is not linear with the rise in temperature.

2.7. Comparative Studies of Water-Filled TES Systems and PCMs

- Mawire et al. (2014) conducted a comparison of sensible heat storage using water and PCM capsules, focusing on solar energy applications [31]. This paper is important for contrasting the energy storage potential of water-filled PET bottles with more advanced PCM technologies.

- Sharma et al. (2009) studied the use of PCMs in TES systems, which offers a different perspective compared to sensible heat storage with water. Including a comparison of water-filled PET bottles and PCM capsules would show the potential trade-offs between sensible and latent heat storage methods [32].

- Sarbu and Sebarchievici (2018) analysed the integration of PCMs and water-based storage mediums in solar heating systems, noting how various materials perform in TES applications [33].

2.8. Environmental and Economic Considerations of Using PET Bottles in TES

- Elias et al. (2019) presented a cost-benefit analysis of using recycled PET bottles in TES systems for residential heating [34]. This study highlighted the economic advantages of using low-cost, recycled materials while considering environmental factors like plastic waste reduction.

- Wu et al. (2024) explored the environmental impact of using recycled materials in TES systems [35]. Their lifecycle assessment of PET bottle usage in thermal storage could complement the sustainability discussions.

- Lopez-Sabiron et al. (2014) examined the potential for incorporating recycled materials in energy storage systems, focusing on lifecycle environmental benefits [36]. This study provides a framework for discussing the environmental viability of using PET bottles in TES applications.

2.9. Case Studies on PET Bottle Use in Solar Heating Systems

- Bharathiraja et al. (2024) presented a case study on using recycled PET bottles in a TES unit for solar water heating systems. Their research demonstrated practical results, including energy savings and system performance improvements [37].

2.10. Future Directions and Technological Improvements

- Lund et al. (2016) provided an overview of future trends in TES technology, emphasizing the integration of low-cost materials like PET bottles in both residential and industrial heating systems [38]. They predict increased interest in using recycled materials due to environmental pressures.

- Sharma et al. (2009) discussed the potential for hybrid TES systems that combine sensible heat storage (water or PET bottles) with phase change materials to improve system efficiency [32]. Their review of hybrid systems offers insights for future studies on optimizing TES systems using a mix of materials.

2.11. Improving TES Efficiency Through Design Modifications

- Dolado et al. (2012) focused on enhancing TES efficiency by optimizing fluid flow, container geometry, and heat exchanger designs [39]. This paper could be compared to studies focusing on water-filled PET bottles, emphasizing how design variations like bottle volume, placement, and arrangement impact system efficiency.

- Salunkhe et al. (2022) presented a study on optimizing HT in solar thermal systems using containers of various shapes and materials, comparing cylindrical, spherical, and other geometrical shapes with plastic materials like PET [40].

2.12. Inlet and Outlet Configurations and Their Effects on TES Systems

- Farid et al. (2004) investigate how inlet and outlet designs impact thermal stratification and HT efficiency,

especially in solar heating systems [41]. This study could help expand on further discussing the impact of intake temperature along with velocity on PET bottle-based systems.

- Singh et al. (2019) explore how different inlet velocities and flow rates affect energy efficiency in large-scale solar water heating systems [42]. Their findings could inform future designs of PET bottle arrangements to optimize for better HT in TES applications.

2.13. Long-Term Durability of PET Bottles in TES Systems

- Salunkhe and Shembekar (2012) focused on the long-term thermal degradation of TES materials, which could apply to PET bottles, raising questions about their durability over extended periods of use [43]. This can be expanded with research evaluating the lifespan of plastic materials in TES environments.
- Reddy et al. (2024) conducted durability testing of TES units made from recycled materials, including PET, in varied climatic conditions [44]. They emphasized the importance of material integrity in real-world solar heating applications, which would be a key aspect for future studies on PET bottles in TES systems.

3. Materials and Methods

The schematic representation of the solar energy heating system, incorporating a TES unit filled with PET bottles, is illustrated in Figure 1. This solar heating system comprises solar collectors, fans, storage units, beverage or water-filled PET bottles, and other necessary installation components.

Fans are utilized to circulate the air, which serves as the working fluid in this setup. The system operates in three distinct phases:

- When the PET bottle requires heating, the air heated by the solar collector is directly delivered indoors.
- If the PET bottle does not require heating, the heated air from the solar collector is directed to another TES unit for storing solar energy.
- When solar energy is unavailable, and the PET bottles need heating, the stored energy is utilized.

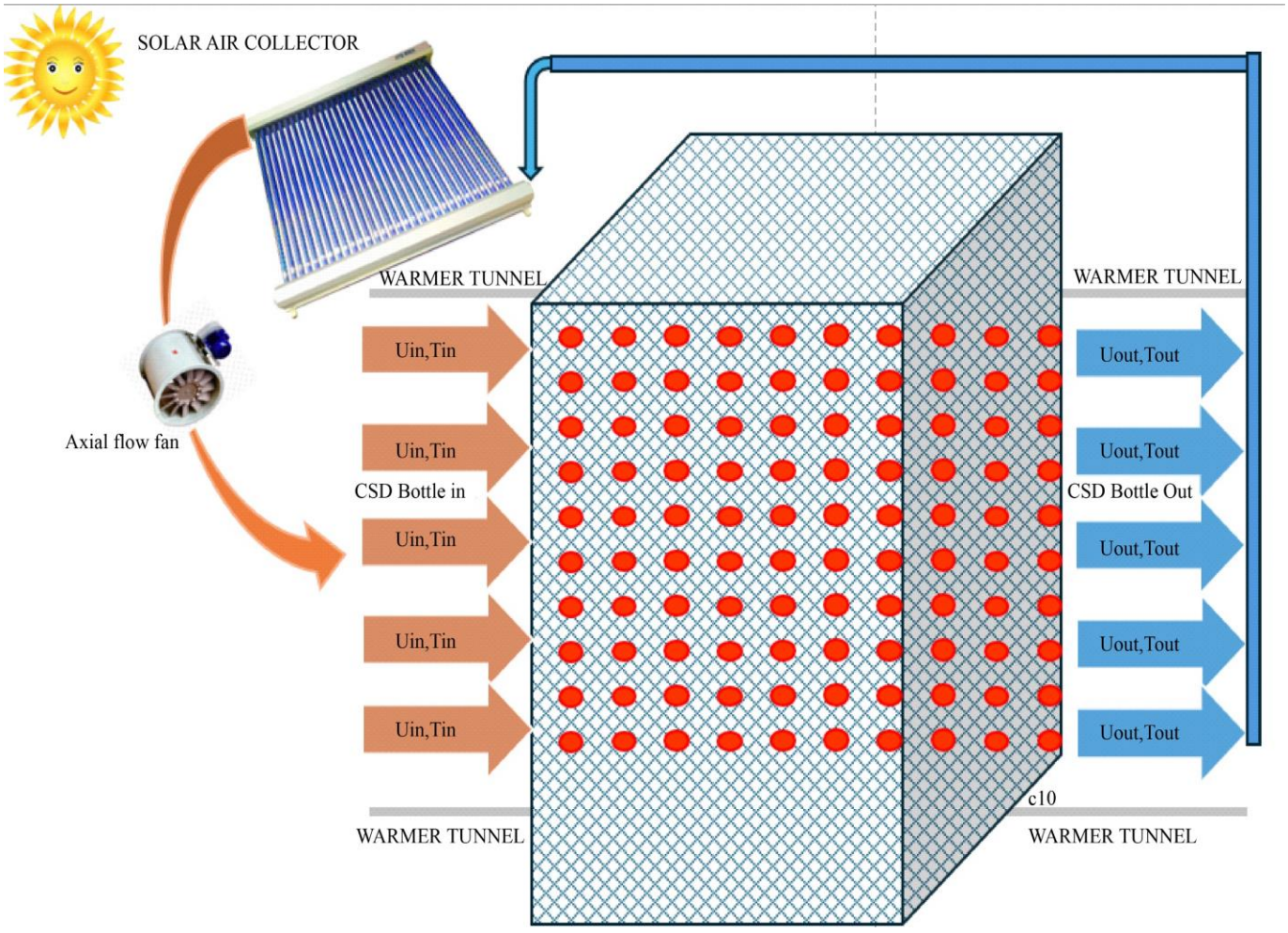

Fig. 1 The schematic view of the system warmer heating tunnel with solar air

Table 1. The dimensions of PET bottles 0.25 to 2.25 *x 10^{-3} m^3* Net Content Capacity

Pack (x10^3 m^3)	Profile	Height (mm)	Brimful Volume (x10^6 m^3)	Average Diameter (mm)	Surface Area (mm^2)	BV/SA (mm)	BV/Height (mm^2)	Brimful to Volume Ratio
0.25	Sting	182	265	54.0	25710	1.03	14.56	1.06
0.33	CAR	187.1	357.0	59.9	32270	1.11	19.08	1.08
0.40	AXL	204.6	424.4	62.2	35927	1.18	20.74	1.06
0.40	GT	193.3	421.9	63.7	35830	1.18	21.83	1.05
0.50	CAR	224.8	523.8	65.5	43050	1.22	23.30	1.05
0.50	GT	197.4	527.4	70.2	40549	1.30	26.72	1.05
0.60	GT	161.2	624.7	73.0	45985	1.36	38.77	1.04
0.60	CAR	237.3	621.3	69.5	48320	1.29	26.18	1.04
0.75	AXL	200.0	778.4	74.0	54539	1.43	38.91	1.04
0.75	CAR	250.0	771.9	74.0	54884	1.41	30.88	1.03
0.75	GT	234.0	773.3	78.0	53356	1.45	33.05	1.03
1.25	CAR	299.0	1291.0	87.6	77386	1.67	43.18	1.03
2.00	CAR	346.0	2046.1	102.9	102690	1.99	59.14	1.02
2.25	CAR	346.0	2306.0	108.1	108910	2.12	66.65	1.02
2.25	AXL	354.5	2316.0	106.7	110514	2.10	65.33	1.03

3.1. System and PET Bottles

This research used 0.25, 0.33, 0.4, 0.5, 0.6, 0.75, 1.25, 2, and 2.25 *x 10^{-3} m^3* PET bottles, often employed in everyday life as the energy transfer or storage container in the TES unit. PET bottles serve as both energy storage containers and heat exchangers. Therefore, the system does not need a HE for the charging and discharging times. The working fluid, air, flows directly over the PET bottles. Figure 2 displays the perspectives and measurements of PET bottles. The performance of PET bottles has been examined by arranging them in various configurations (inline as well as staggered) and locations. Furthermore, various intake temperatures and velocities have been examined to ascertain the system's response under varied operational circumstances. Theoretical heat transport evaluations have been conducted. Empirical formulae have been used to calculate the system's stored energy quantity. During the computations, PET bottles have been treated as cylindrical objects with a specified diameter (d) and height (H), as shown in Table 1.

4. HT Analysis and Storage

Table 2 presents a schematic representation of the HT unit. It contains 0.25, 0.33, 0.4, 0.5, 0.6, 0.75, 1.25, 2, 2.25 x 10-3 m3 PET bottles arranged in a straight line and staggered pattern, respectively. The cumulative HT or storage capacity amounts inline arranged 924-2079,648-1499,358-819 with bottle Gap 0.25d, 0.5d, 1d respectively, Staggered 892-1935, 621-1377, 338-729 with bottle Gap 0.25d, 0.5d, 1d respectively. The PET bottles have been arranged in warmer 0.25 x 10-3 m3 88 x 42 grids on a warmer moving chain. Specifically, there are a total of 88 bottles arranged in columns and 42 rows on a horizontal plane. The uniformity of the bottle arrangement in the horizontal plane was considered, given its significant influence on HT analysis. This standardized arrangement was applied across all bottle types to enable a consistent comparison of HT along with HT performance.

In Figures 2a, 2b, 2c, and 2d, no vertical arrangement of bottles has been altered to achieve a total HT or storage capacity. Three types of Inline arrangements are below with spacing 0.25d, 0.5d, and 2.25d. This study includes single arrays for all sets of bottles from 0.25 to 2.25 x 10-3 m3 in the orientation as above in the heating or warming tunnel. The quantity of 0.25 x 10-3 m3 bottles is 3696, while the quantity of 2.25 x 10-3 m^3 bottles is 924, each with a gap of 0.25 times the diameter of the bottle. The quantity of 0.25 x 10-3 m3 bottles is 2590, while the quantity of 2.25 x 10-3 m3 bottles is 629, each with a gap of 0.5 times the diameter of the bottle. The quantity of 0.25 x 10-3 m3 bottles is 1430, while the quantity of 2.25 x 10-3 m3 bottles is 351 each with a gap of 1 times the diameter of the bottle.

Three types of Staggered arrangements are below with spacing 0.25d,0.5d, and d. This study includes single arrays for all sets of bottles from 0.25 to 2.25 $x\ 10^{-3}\ m^3$ in the orientation. The quantity of 0.25 $x\ 10^{-3}\ m^3$ bottles is 3567, while the quantity of 2.25 $x\ 10^{-3}\ m^3$ bottles is 860, each with a gap of 0.25 times the diameter of the bottle. The quantity of 0.25 $x\ 10^{-3}\ m^3$ bottles is 2482, while the quantity of 2.25 $x\ 10^{-3}\ m^3$ bottles is 576, each with a gap of 0.5 times the diameter of the bottle. The quantity of 0.25 $x\ 10^{-3}\ m^3$ bottles is 1350, while the quantity of 2.25 $x\ 10^{-3}\ m^3$ bottles is 312, each with a gap of 1 times the diameter of the bottle.

Table 2. Warming Tunnel capacity with arrangements bottle spacing 0.25d, 0.5d, d of PET bottles arrangements inline and staggered

Pack	Profile	Average Diameter	In line Arrangement														
			0.25					0.5					1				
$*10^{-3}$ m^3		mm	Contraction Ratio	Bottles along width	Bottles along Length	No bottles in Warmer	Capacity in $*10^{-3}$ m3	Contraction Ratio	Bottles along width	Bottles along Length	No of bottles in Warmer	Capacity in $*10^{-3}$ m3	Contraction Ratio	Bottles along width	Bottles along Length	No of bottles in Warmer	Capacity in $*10^{-3}$ m3
0.25	Sting	54.0	0.20	42	88	3696	924	0.33	35	74	2590	648	0.50	26	55	1430	358
0.33	CAR	59.9	0.20	38	80	3040	1003	0.33	32	66	2112	697	0.50	24	50	1200	396
0.40	AXL	62.2	0.20	37	77	2849	1140	0.33	31	64	1984	794	0.50	23	48	1104	442
0.50	CAR	65.5	0.20	35	73	2555	1278	0.33	29	61	1769	885	0.50	22	45	990	495
0.60	CAR	69.5	0.20	33	69	2277	1366	0.33	27	57	1539	923	0.50	20	43	860	516
0.75	CAR	74.0	0.20	31	64	1984	1488	0.33	26	54	1404	1053	0.50	19	40	760	570
1.25	CAR	87.6	0.20	26	54	1404	1755	0.33	22	45	990	1238	0.50	16	34	544	680
2.00	CAR	102.9	0.20	22	46	1012	2024	0.33	18	38	684	1368	0.50	14	29	406	812
2.25	CAR	108.1	0.20	21	44	924	2079	0.33	17	37	629	1415	0.50	13	27	351	790

Staggered Arrangement														
0.25					0.5					1				
Contraction Ratio	Bottles along width	Bottles along Length	No of bottles in Warmer	Capacity in $*10^{-3}$ m3	Contraction Ratio	Bottles along width	Bottles along Length	No of bottles in Warmer	Capacity in $*10^{-3}$ m3	Contraction Ratio	Bottles along width	Bottles along Length	No of bottles in Warmer	Capacity in $*10^{-3}$ m3
0.99	41	87	3567	892	0.99	34	73	2482	621	1.00	25	54	1350	338
0.99	37	79	2923	965	0.99	31	65	2015	665	1.00	23	49	1127	372
0.99	36	76	2736	1094	0.99	30	63	1890	756	1.00	22	47	1034	414
0.99	34	72	2448	1224	0.99	28	60	1680	840	1.00	21	44	924	462
0.99	31	67	2077	1039	0.99	26	55	1430	715	1.00	19	41	779	390
0.99	30	63	1890	1418	0.99	25	53	1325	994	1.00	18	39	702	527
0.99	30	63	1890	1418	0.99	25	53	1325	994	1.00	18	39	702	527
0.99	25	53	1325	1656	0.99	21	44	924	1155	1.00	15	33	495	619
0.99	21	45	945	1890	1.00	17	37	629	1258	1.00	13	28	364	728
0.99	20	43	860	1935	1.00	16	36	576	1296	1.00	12	26	312	702

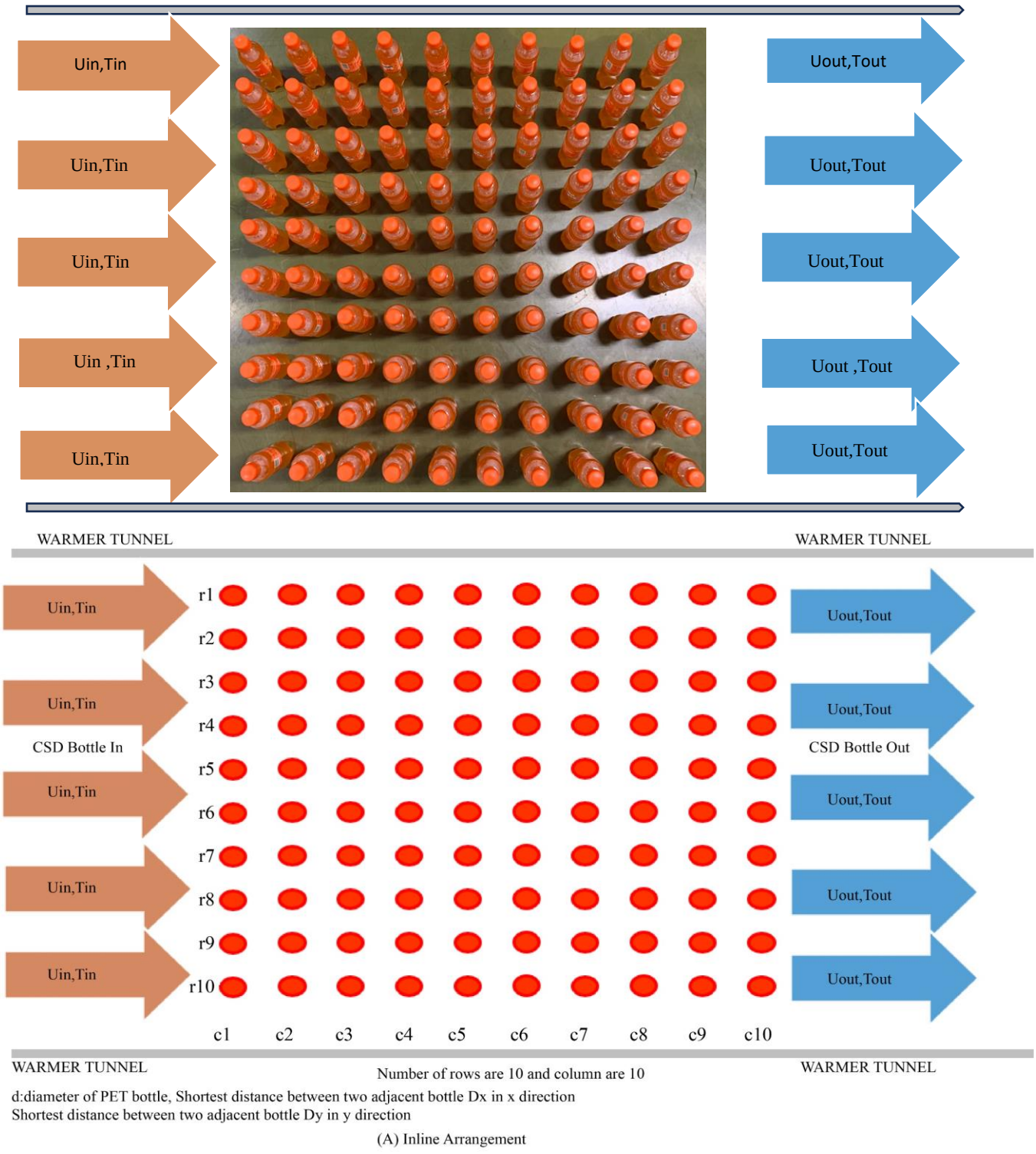

Fig. 2a and 2b: The arrangements of PET bottles inline and flow direction air and bottle

Figures 2a, 2b, 2c and 2d display the spatial positioning of PET bottles in the horizontal plane. PET bottles have been arranged in two distinct configurations on a flat surface. These are examples of inline (Figure 2a and 2b) and staggered (Figure 2c and 2d) configurations. The spacing between the bottles has been measured at 0.25 times the diameter (d), 0.50 times the diameter, and 1.00 times the diameter in both the rows and columns. In addition to the bottle arrangement, the impact of air intake velocity and temperature on TES performance has been examined.

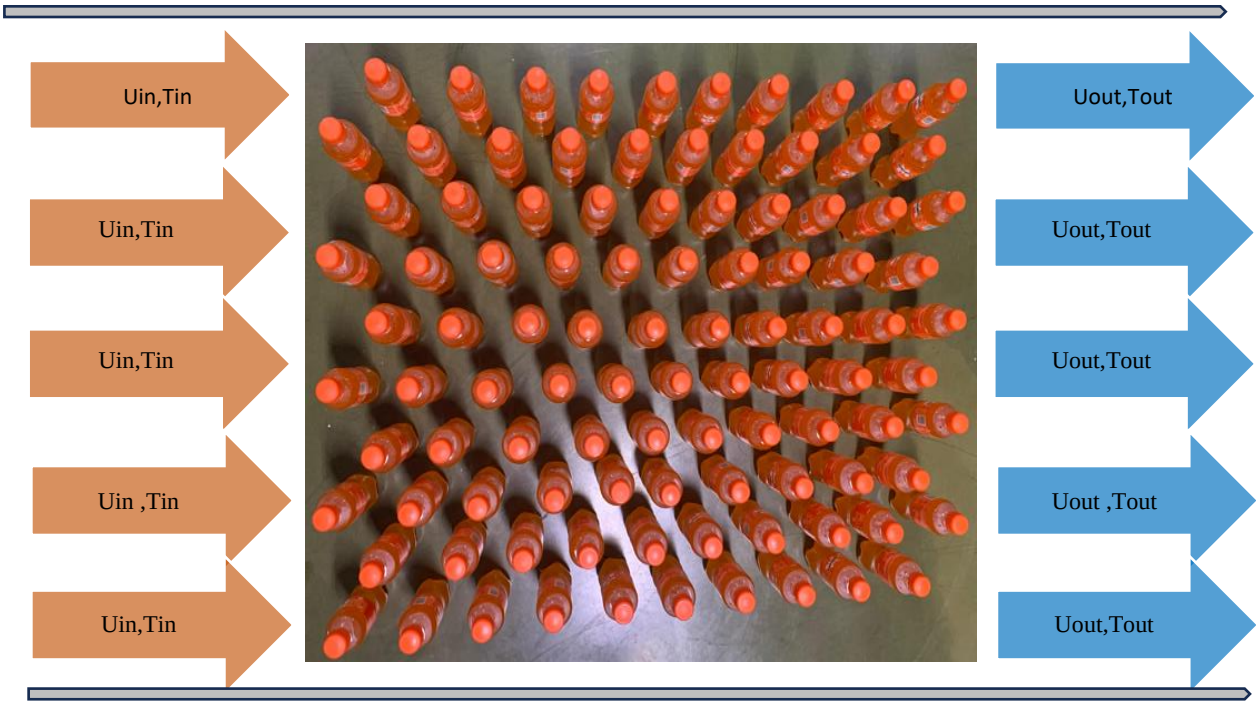

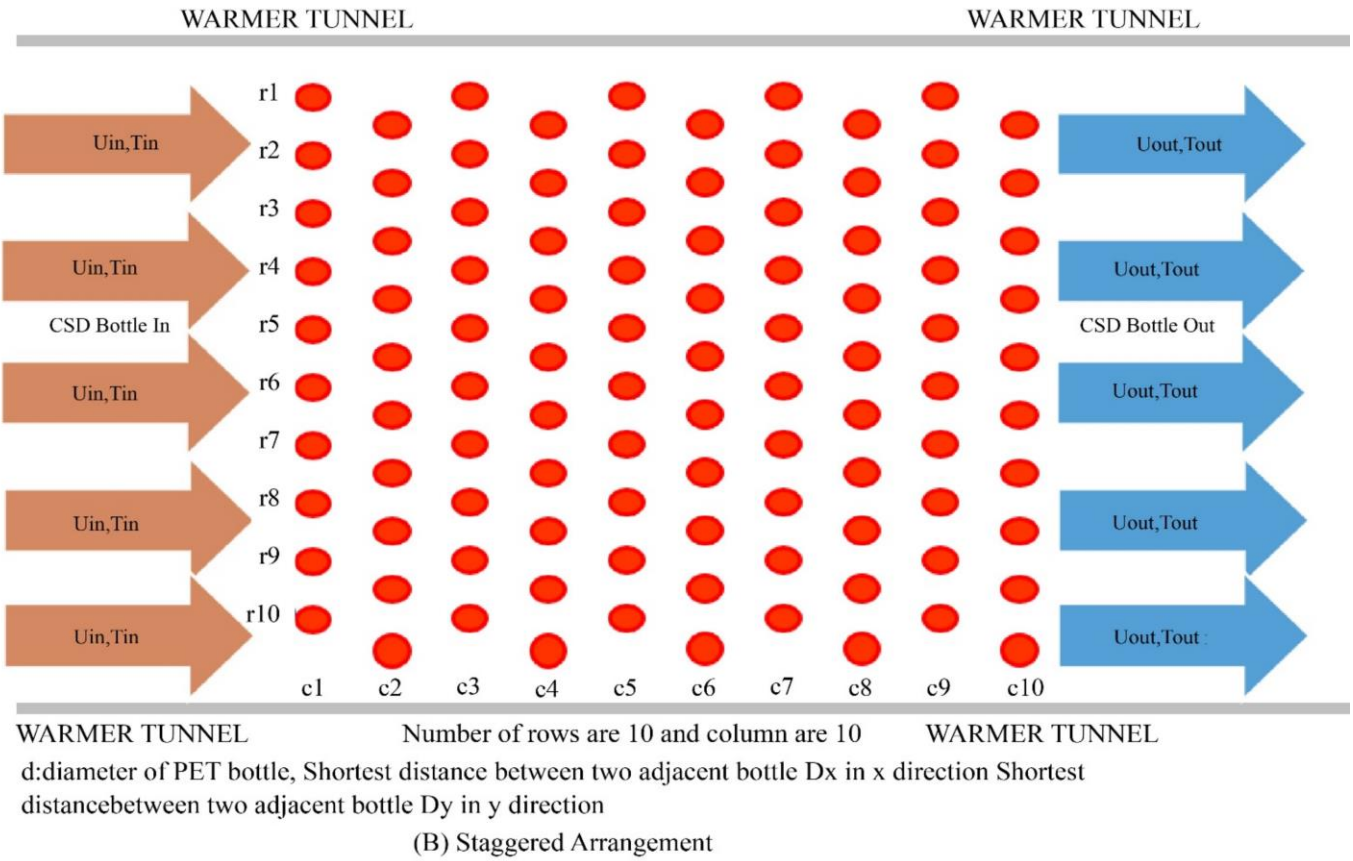

d:diameter of PET bottle, Shortest distance between two adjacent bottle Dx in x direction Shortest distancebetween two adjacent bottle Dy in y direction

(B) Staggered Arrangement

Fig. 2c and 2d: The arrangements of PET bottles staggered and flowed in the direction of the air bottle

The maximum velocity in a PET bottle, especially in an inline or staggered arrangement, can be derived from fluid dynamics principles like continuity and Bernoulli's equations.

4.1. Continuity Equation

The continuity equation relates the flow velocity to the available cross-sectional area

$$A_1 \cdot V_1 = A_2 \cdot V_2 \quad (1)$$

A_1, A_2 = cross-sectional areas before and between PET bottle bank, V_1, V_2= velocities at respective cross-sections. In PET bottle banks, the flow area between the bottles decreases, leading to an increase in velocity.

4.2. Maximum Velocity in PET Bottle as Tube Bank

For a bottle bank, the maximum velocity Vmax is typically calculated using the ratio of free-flow area to the minimum cross-sectional area available for flow between the tubes. The formula for maximum velocity can be expressed.

$$V_{max} = \frac{V\infty}{\sigma} \quad (2)$$

Where,

V∞= free-stream velocity (the velocity of fluid approaching the bottle bank),

σ = contraction ratio, which is the ratio of free-flow area to the minimum area available between the tubes.

The contraction ratio σ depends on the arrangement of the tubes:

4.2.1. Inline Arrangement

$$\sigma_{inline} = 1 - \frac{d}{d+Dx} \quad (3)$$

D is the PET bottle diameter, and Dx is the transverse pitch (the distance between the adjacent bottle's surface in the flow direction).

Lower HTs are due to less turbulence, weaker mixing, and more significant boundary layer growth. Lower pressure drop is less efficient, especially in the downstream rows where wake regions dominate.

4.2.2. Staggered Arrangement

$$\sigma_{staggered} = 1 - (\frac{d}{d+Dx})(\frac{d}{d+Dy}) \quad (4)$$

Dy is the longitudinal pitch (distance between adjacent bottle surfaces in the perpendicular direction to the flow).

Higher HT is due to increased turbulence, better mixing, and more frequent boundary layer disruption. Higher pressure drops are more efficient, as turbulent eddies bring fresh fluid to the surface and enhance convective HT.

Thus, the staggered arrangement is preferred when higher HT rates are desired, although it comes with the cost of a higher pressure drop. The inline arrangement is used when minimizing pressure drop, which is more important than maximizing HT.

The values of the HT coefficient h for different air velocities are based on a common empirical relationship for turbulent flow.

$$h \propto v^n \quad (5)$$

Where n is typically between 0.5 and 0.8 for turbulent flow. Assumed n=0.8 is a reasonable assumption for air flowing over PET bottles. However, the actual value of h will depend on many factors, such as the shape and surface of the PET bottles, The arrangement of the bottles (e.g., inline or staggered), The nature of the airflow (whether it's laminar or turbulent), The Reynolds number (Re), which depends on air velocity, bottle size, and air properties.

The Nusselt number (Nu), which is related to h through the formula

$$Nu = \frac{h \cdot d}{k} \quad (6)$$

The Nusselt number (Nu) relates the convective HT coefficient h to the thermal conductivity of the fluid k, where k is the thermal conductivity of air and d is the characteristic length (e.g., bottle diameter).

To verify whether the values of h are correct for specific cases, it would be ideal to use correlations or empirical data from HT studies for cylindrical objects (such as PET bottles) in cross-flow air streams. One of the most common approaches for forced convection over cylinders is using empirical correlations for the Nusselt number Nu, such as:

$$Nu = C \cdot Re^m \cdot Pr^n \quad (7)$$

The Reynolds number (Re) is a dimensionless quantity used in fluid mechanics to characterize the flow regime of a fluid. It is the ratio of inertial forces to viscous forces. It indicates whether the flow is laminar (Re < ~2000) or turbulent (Re > ~4000), with transitional flow in between. The Prandtl number (***Pr*** is another dimensionless quantity used in heat transfer analysis. It represents the ratio of momentum diffusivity (viscous diffusion) to thermal diffusivity.

The HT analysis for the flow of heated air across the PET bottle array was calculated using equations developed by Grimson (1937) [45].

Where C and m are constant coefficients taken from the table, which is situated in [46], and n is assumed 1/3 based on the flow regime (laminar or turbulent).

To calculate h, require the Reynolds number Re, the Prandtl number Pr., and the thermal conductivity of air k at the given temperature (approximately 0.026 W/m·K at room temperature). The Reynolds number is given by

$$Re = \frac{\rho \cdot V\infty \cdot d}{\mu} \quad (8)$$

Where: ρ is the density of air (about 1.2 kg/m³ at room temperature), $V\infty$ is the velocity of air (0.5 m/s, 2 m/s, 5 m/s, 10 m/s), d is the diameter of the bottle (Different Stock keeping Units have different diameter),μ is the dynamic viscosity of air (approximately 1.81×10^{-5} kg/m).

An empirical correlation for Nu for cylinders in cross-flow [45], typically for $10^4<Re<10^5$

$$Nu = 0.3 + 0.62Re^{0\cdot5}Pr^{1/3} \quad (9)$$

Where Pr the Prandtl number for air is approximately 0.71calculate h for the different air velocities.

In this scenario, where bottles are moving on a conveyor and are continuously exposed to hot air, new bottles enter at 280 K and exit at 296 K. Account for the steady-state HT between the air and the moving bottles, considering the following factors: Convective HT between the air and the bottles, Mass Flow Rate of Bottles moving on the conveyor, Energy Balance to determine how much heat is transferred to each bottle as it moves through the system.

4.3. Convective HT Rate

The heat transferred from the air to each bottle is given by the convective HT equation:

$$Q_{conv} = h \cdot A \cdot (T_{air} - T_{bottle}) \quad (10)$$

Where,

Q_{conv} is HT rate (W),

A is the surface area of each bottle (m²),

h is convective HT coefficient (W/m²·K),

T_{air} is the temperature of the air (hot air temperature, assumed constant),

T_{bottle} temperature of the bottle (changes as it moves through the system)

4.4. Energy Balance on a Bottle

For each bottle, the heat transferred from the air will increase the temperature of the water inside. The energy balance for each bottle Q_{conv}, rate of HT to the bottle (W):

$$Q_{conv} = m \cdot C_w \cdot \frac{dT}{dt} \quad (11)$$

Where,

m is the mass of water inside the bottle (kg),
C_w, specific heat capacity of water (J/kg·K),
dT/dt, the rate of change in the temperature of the water in the bottle.

The temperature change from 280 K to 296 K as the bottles move through the system will depend on the HT rate and the time the bottles spend in the air stream.

4.5. Mass Flow Rate of Bottles

If the bottles are moving on a conveyor, the mass flow rate of the bottles can be calculated by:

$$\dot{m} = \rho_{water} \cdot V_{bottle} \cdot \frac{N}{t_{conveyor}} \quad (12)$$

Where,

$\dot{m}$ is the mass flow rate of the bottles (kg/s)
ρ_{water} is density of water (kg/m³),
V_{bottle}, volume of water in each bottle (m³),
N is the number of bottles on the conveyor at a time,
$t_{conveyor}$ is time for each bottle to move through the air stream (s).

4.6. Energy Balance for the System

The energy added to each bottle by the hot air is the amount required to raise its temperature from 280 K to 296 K. Using the formula for energy required to change the temperature of a mass of water:

$$Q = m \cdot c \cdot (T_{exit} - T_{inlet}) \quad (13)$$

Where Q is heat added to each bottle (J), M is the mass of water in each bottle (kg), c is the specific heat capacity of water (4186 J/kg), T_{exit}=296 K, and T_{inlet}=280 K.

4.7. HT over Time

To account for the fact that the bottles are moving, need to integrate the HT over the time the bottles are in contact with the air:

$$Qconv = \int_0^{t_{total}} h \cdot A \cdot (T_{air} - T_{bottle}(t))dt \quad (14)$$

Where t_{total} is the total time the bottles spend in the air stream, the temperature of the bottles changes with time as they move through the system.

4.8. Equation for Temperature Change of Moving Bottles

The rate of temperature change of the bottles as they move through the system can be modelled by the lumped capacitance model (assuming uniform temperature within the bottles) [45]:

$$\frac{dT_{bottle}}{dt} = \frac{h\cdot A}{m\cdot c} \cdot (T_{air} - T_{bottle}) \quad (15)$$

This is a first-order differential equation that describes how the temperature of the bottles changes as they move through the air stream. The solution of this equation is:

$$T_{bottle}(t) = T_{air} - (T_{air} - T_{inlet}) \cdot e^{\frac{-h\cdot A\cdot t}{m\cdot c}} \quad (16)$$

Where,
T_{bottle} (t) is the temperature of the bottle at time t,
T_{air} is the temperature of the air,
h is convective HT coefficient (W/m²·K),
A is the surface area of the bottle (m²),
m, mass of water in the bottle (kg),
C is specific heat capacity of water (J/kg·K) [46] [47].

4.9. Conveyor Speed and Bottle Residence Time

The total time t_{total} that each bottle spends in the air stream depends on the speed of the conveyor and the length of the air stream section:

$$t_{total} = \frac{L}{v_{conveyor}} \quad (17)$$

Where L, length of the air stream section (m),$v_{conveyor}$, speed of the conveyor (m/s).

5. Result and Discussion

This study explores the heat absorbed by PET bottles filled with chilled beverages or water. The bottles were arranged on a conveyor belt within a heating tunnel, utilizing both inline and staggered patterns. The spacing between the bottles in rows and columns was set to 0.25d, 0.50d, and 1d. Furthermore, the impact of intake temperature along with intake velocity on the TES efficiency was analysed. The parameters considered in this work are outlined in Table 1, and their influence on the amount of stored energy was calculated.

The Impact of Bottle Size and Measurements - the current investigation used 0.25, 0.33, 0.4, 0.5, 0.6, 0.75, 1.25, 2, 2.25 *x 10^{-3} m^3* PET bottles, often employed in everyday life. The arrangement and quantity of bottles in a horizontal plane have a considerable impact on heat transmission in the warmer Tunnel. Therefore, PET bottles have been arranged in multiple configurations on a horizontal plane. No bottles in the vertical orientation vary as considered in a horizontal plane on the conveyor, as the quantity of PET bottles in the vertical plane has very little impact on the HT study. The relationship between the capacity of PET bottles and the quantity of stored energy.

(Q_{stored}) is shown in Figure 5 for eighteen distinct situations and 15 SKUs. According to Figure 5, the quantity of stored energy decreases as the capacity of the bottle grows. This is because the diameter of the bottle increases as the volume increases. Therefore, the maximum Reynolds number increases when the bottle diameter increases. A rise in Reynolds number has resulted in an increase in both Nusselt number and average HT coefficient. While the average HT coefficient has increased as the container diameter increases, the quantity of stored energy has dropped. Due to the growing bottle diameter, the overall heat transmission surface area for the bottles has been reduced.

The graph presents a 3D surface plot showing the heat transferred to PET bottles, measured in kilowatts (kW), based on various bottle configurations and system parameters. The x-axis represents different bottle arrangements, such as "Inline" and "Staggered," along with corresponding bottle sizes (ranging from 0.25 to 2.25 *x 10^{-3} m^3*). The arrangement types indicate how bottles are positioned in the system, which can influence the HT process. The y-axis highlights different operational parameters or variables (Sting, Carolina, Axl, Grip Tight), potentially representing factors like inlet velocity, flow type, or heat source characteristics.

Table 3. Studied parameters

Parameters	Value
Bottle volume *x 10^{-3} m^3*	0.25, 0.33, 0.4, 0.5, 0.6, 0.75, 1.25, 2, 2.25
Arrangements	Inline, staggered
Dy, longitudinal distance between adjacent bottles surface in the perpendicular direction to the flow	0.25d, 0.5d, d
Dx, the transverse distance between the adjacent bottles' surfaces in the flow direction	0.25d, 0.5d, d
Inlet velocity (m/s)	1, 2, …, 9, 10,11
Inlet temperature,	303,308,313,318,323,328 K

The z-axis represents the HT values, grouped into color-coded ranges: from 0-10 kW (shown in orange and blue) to 60-70 kW (shown in green and purple). The graph demonstrates that certain configurations, especially those with larger bottle volumes or staggered arrangements, tend to show higher HT (50-70 kW). This suggests better thermal efficiency under these conditions. Conversely, smaller volumes or inline configurations tend to have lower heat absorption, as seen in the lower ranges (0-10 kW).

5.1. The Effects of Temperature and Air Inlet Velocity

The variation in stored energy as a function of the input velocity is shown in Figure 4. The graph illustrates the impact of intake air velocity on the thermal energy performance of a 0.25 *x 10^{-3} m^3* Sting bottle (with a diameter of 54 mm and a height of 182 mm) in a heating tunnel. The bottle spacing is set at 0.25 times the bottle diameter. The x-axis shows the inlet air velocity (1 to 11 m/s), the y-axis on the left represents the convective HT rate (in kW), and the y-axis on the right shows the Reynolds and Nusselt numbers.

The HT rates for two configurations—In line and Staggered are presented. As the inlet air velocity increases, both configurations show a rise in HT rates, with the staggered arrangement generally providing higher HT. The Nusselt Number and Reynolds Number also increase with velocity, indicating improved HT due to enhanced convective effects.

The Convective HT Coefficient shows a steady rise, indicating that as air velocity increases, the efficiency of HT improves. This graph highlights the impact of higher airflow rates on increasing HT rates, particularly for staggered bottle configurations, which are more thermally efficient than inline arrangements.

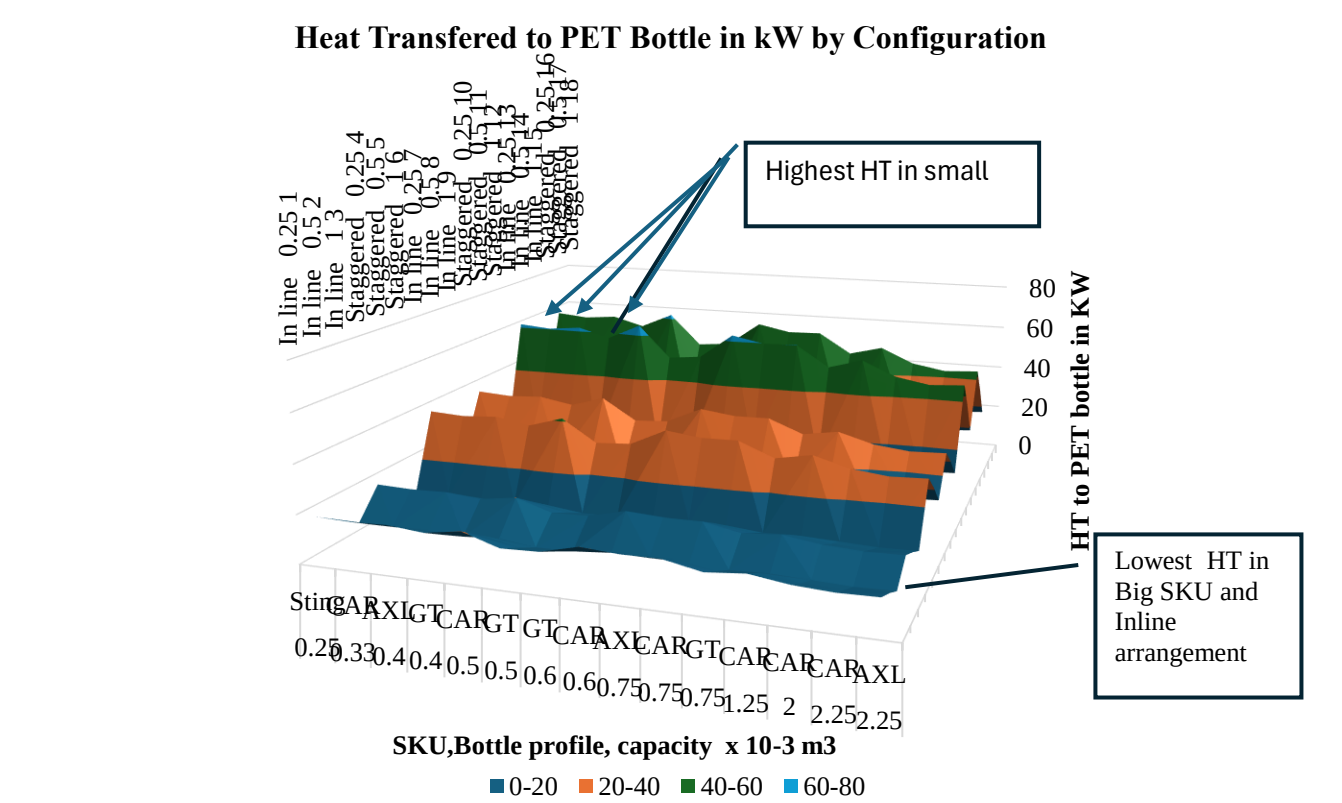

Fig. 3 The impact of PET bottle volume and configuration on the Heat transferred

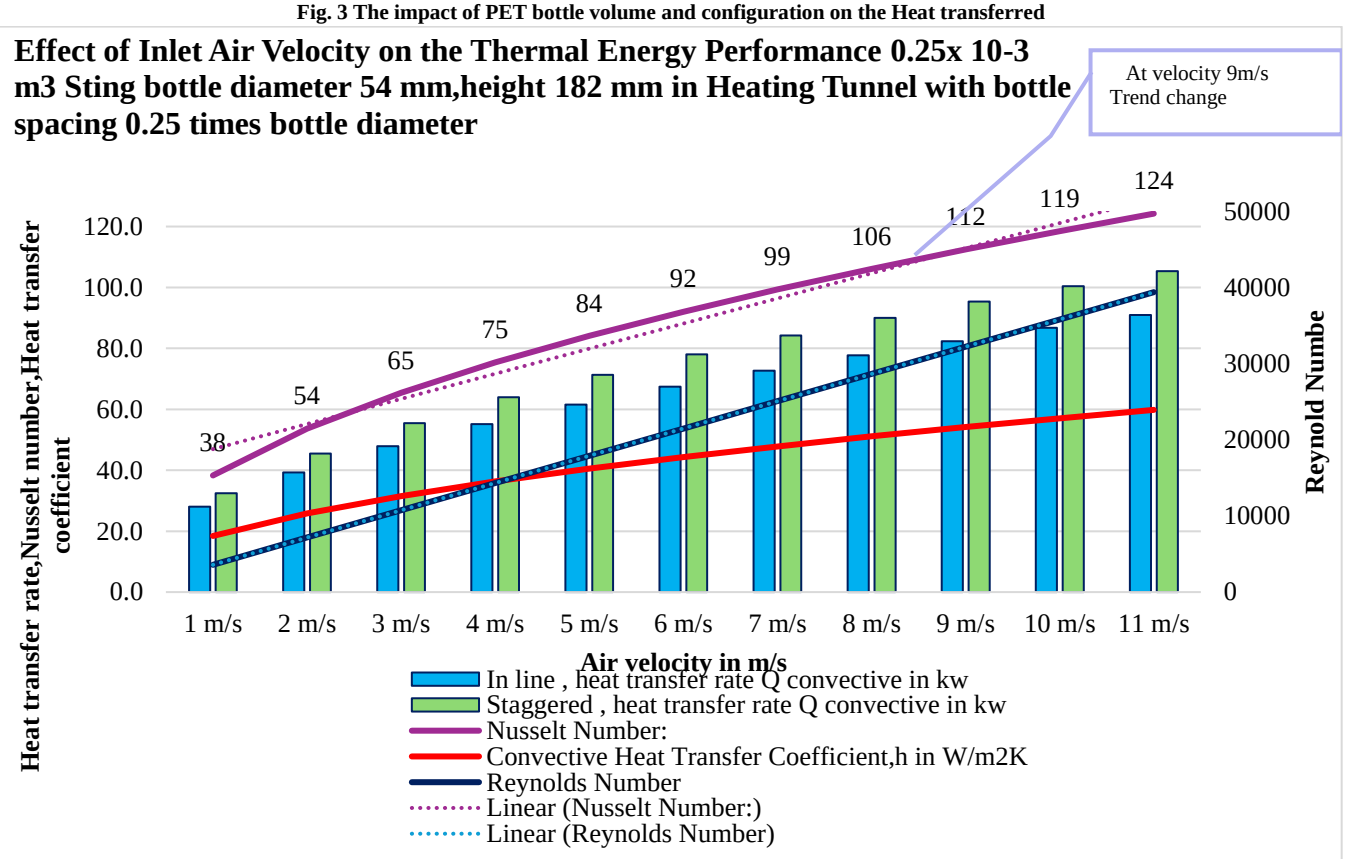

Fig. 4 The impact of intake velocity on sensible TES's thermal performance

Figure 5 shows the effect of intake air velocity on the thermal energy performance of a 2.250 *x* 10^{-3} m^3 Carolina bottle (diameter: 108.1 mm, height: 346 mm) in a heating tunnel, with bottle spacing set at 0.25 times the bottle diameter. The x-axis indicates the inlet air velocity (from 1 to 11 m/s), the y-axis on the left shows the convective HT rate (kW), and the y-axis on the right represents the Nusselt and Reynolds numbers.

The HT rate increases as inlet air velocity rises for both the inline and staggered configurations. The staggered configuration consistently results in a higher HT rate compared to the inline arrangement, suggesting better thermal efficiency at all air velocities.

The Nusselt Number and Reynolds Number also increase with air velocity, indicating enhanced convective HT. The Convective HT Coefficient shows a more gradual rise but follows a similar trend, confirming that higher velocities improve HT. This graph demonstrates larger bottle sizes like the 2.250 x 10-3 m3. Carolina bottles require higher airflow to achieve efficient HT, with the staggered arrangement offering superior thermal performance.

The graph in Figure 6, illustrates the impact of bottle size along with airflow velocity on the thermal energy performance of two types of bottles 0.250 *x* 10^{-3} m^3 Sting and 2.250 *x* 10^{-3} m^3 Carolina—arranged in a staggered configuration within a heating tunnel. The graph compares the convective HT rate (Q in kW) for each bottle type at varying air velocities from 1 to 11 m/s. As the airflow velocity increases, the HT rate also increases for both bottles, with the 0.250 *x* 10^{-3} m^3 Sting bottle consistently showing a higher HT rate than the larger 2.250 *x* 10^{-3} m^3 Carolina bottle across all velocities.

The total surface area for each bottle type is also depicted, with the larger Carolina bottle having a greater surface area but lower HT performance compared to the Sting bottle. The graph also includes the Reynolds number for each bottle, which increases with airflow velocity and indicates the flow dynamics around the bottles.

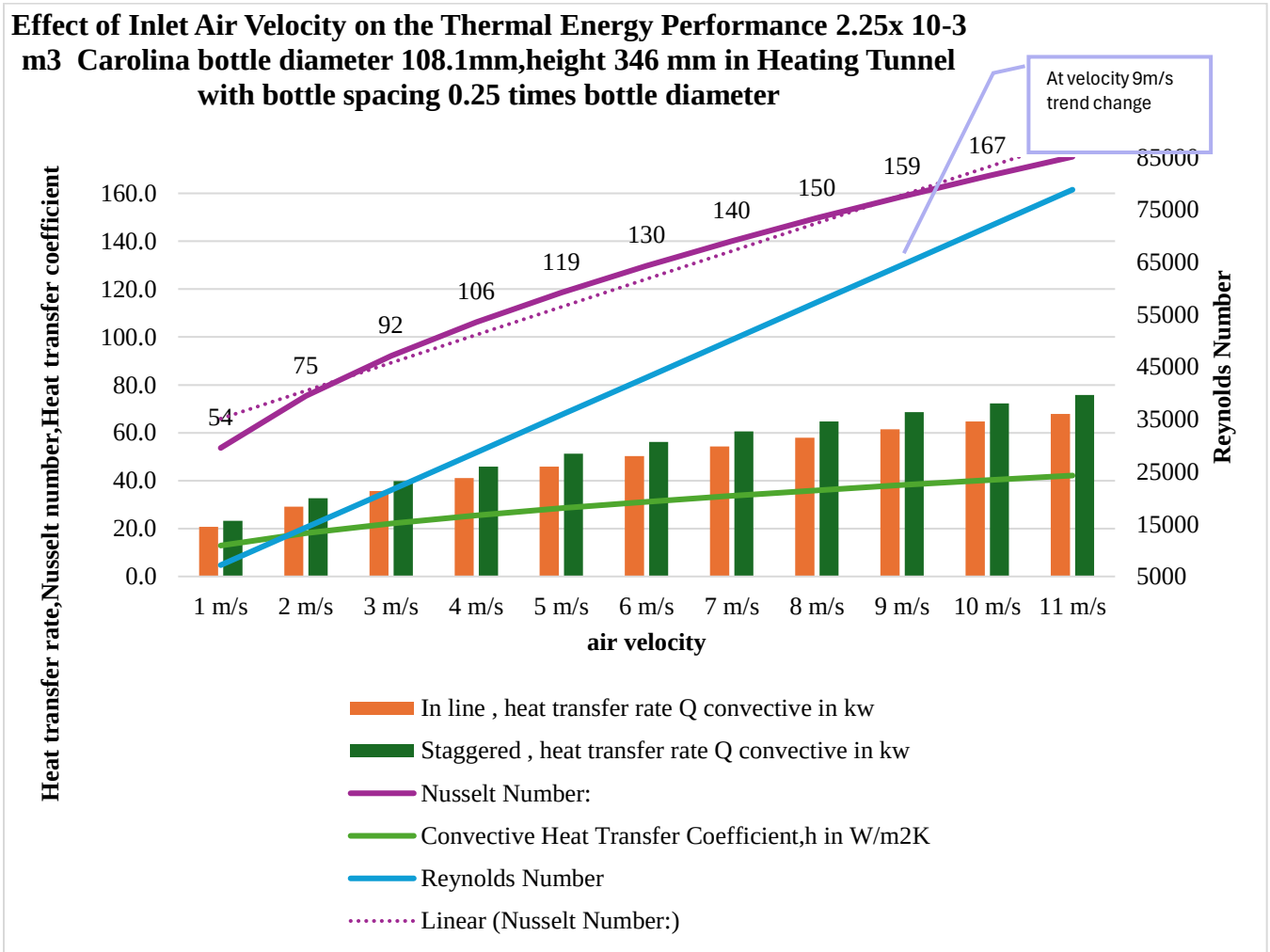

Fig. 5 The effect of inlet velocity, Bottle size 2.25 x 10-3 m3 on **thermal performance of sensible TES**

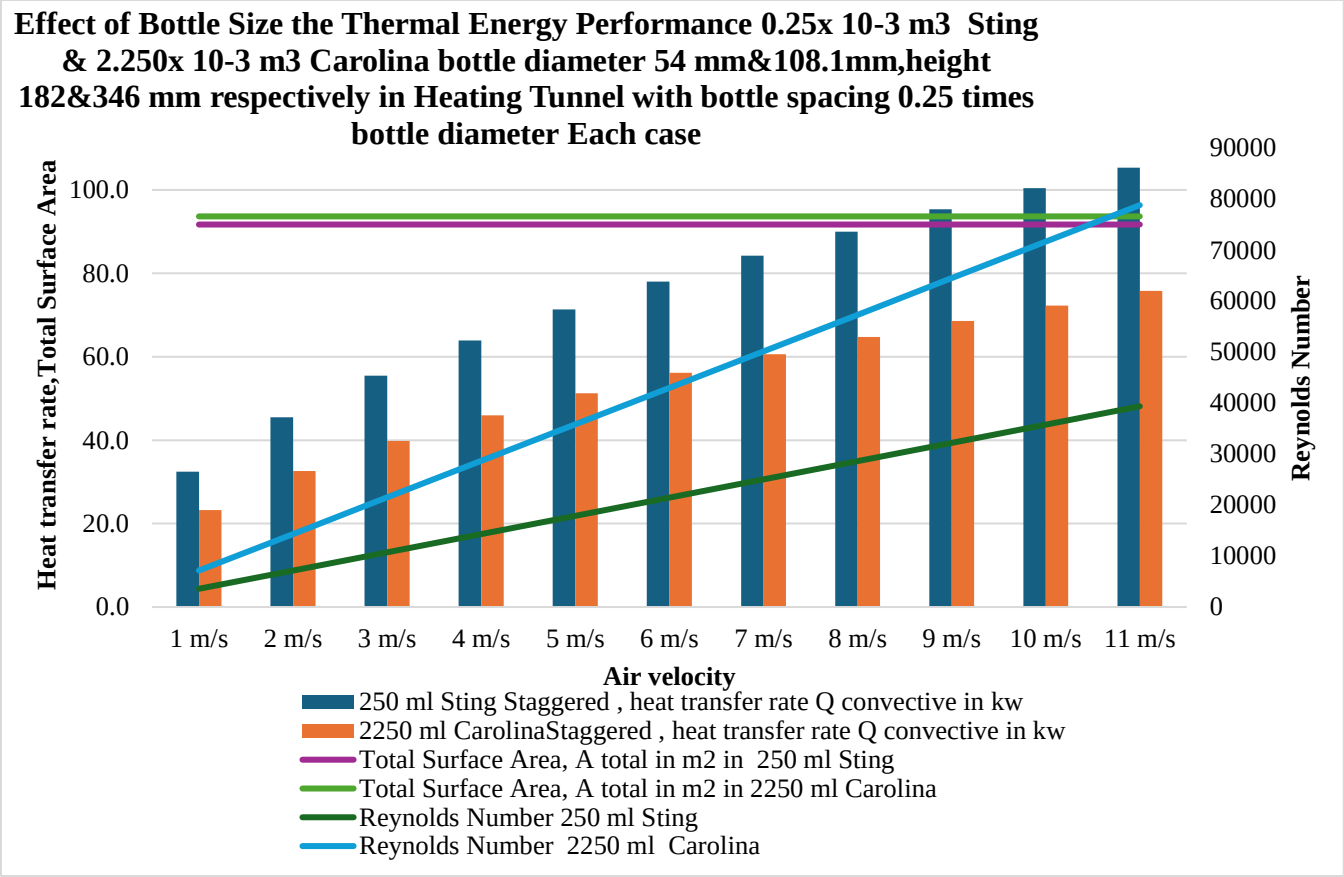

Fig. 6 The effect of inlet velocity, Bottle size 0.25 vs 2.25 x 10-3 m3 on thermal performance of sensible TES

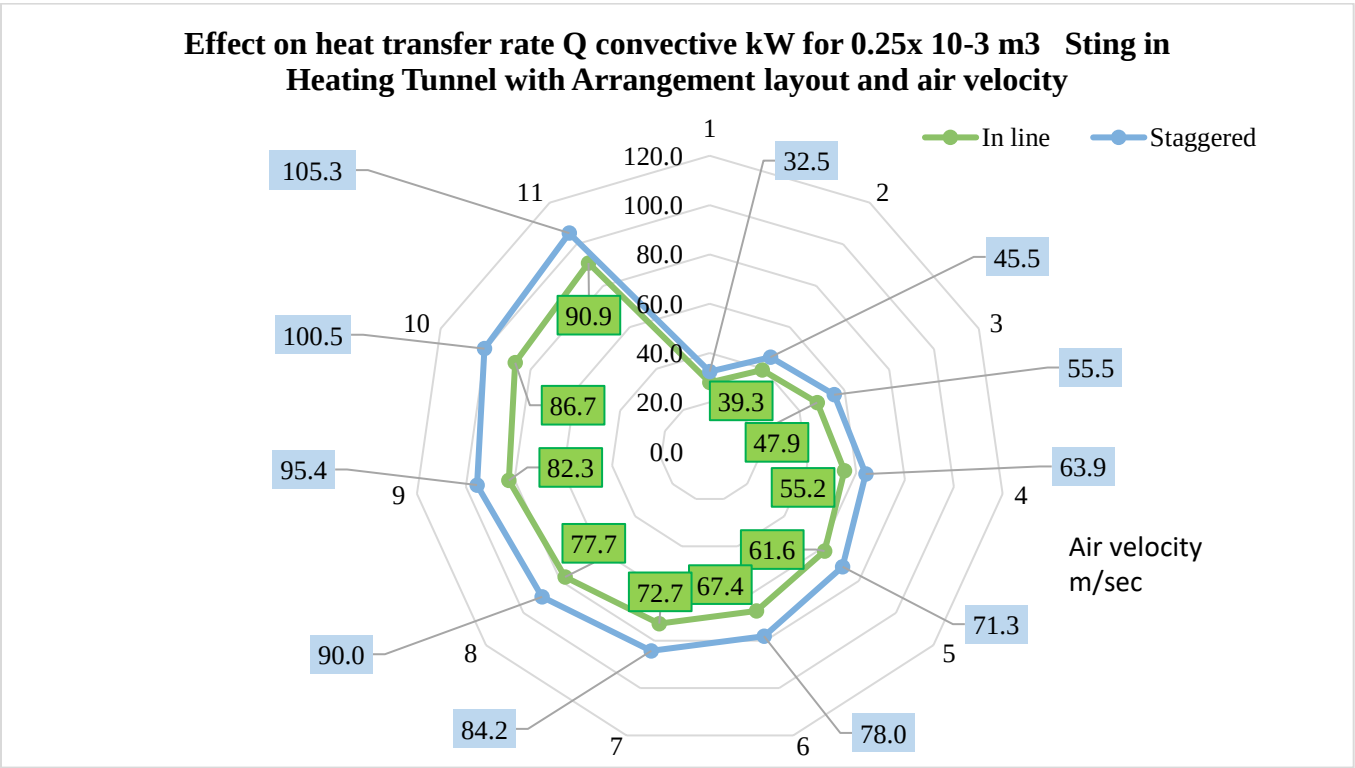

Fig. 7 The effect of arrangement layout and air velocity on the thermal performance of sensible TES

This spider web graph Fig 7 presents the convective HT rate (Q, in kW) for a 0.25 *x* 10^{-3} m^3 Sting bottle arranged in two configurations: inline and staggered, spanning a range of air velocity from 1 to 11 m/s. The data is divided based on the spacing of the bottles, set at 0.25 times the bottle diameter (d).

Key observations:

1. The staggered configuration consistently shows a higher HT rate than the inline configuration at all air velocities.
2. At 1 m/s, the HT rate is 28.0 kW for the inline arrangement, increasing to 32.5 kW for the staggered configuration.
3. As air velocity increases, the HT rate rises significantly in both configurations, reaching 90.9 kW (inline) and 105.3 kW (staggered) at 11 m/s.
4. The difference in HT rates between the two configurations becomes more pronounced as the air velocity increases, indicating that the staggered arrangement benefits more from higher airflows.

5.1.1. Analysis of Data: Relationship between Heat Transfer Coefficient and Bottle Size

This data highlights the role of bottle arrangement and air velocity in enhancing the convective HT performance in thermal processes involving small PET bottles.

Figure 8 explores the relationship between PET bottle diameter, air velocity, and the convective HT coefficient (h in W/m²K) for various PET bottle sizes, ranging from 0.25 to 2.25 *x* 10^{-3} m^3. Three air velocities are considered: low (0.5 m/s), medium (2 m/s), and high (5 m/s). The HT coefficient generally increases with airflow velocity but decreases as bottle size increases.

The HT coefficient is the lowest across all bottle sizes at low air velocity, with values ranging between 10 and 20 W/m²K. As bottle diameter increases, the convective HT reduces slightly, reflecting minimal air interaction for larger bottles at this velocity.

The medium air velocity shows a moderate rise in the HT coefficient, ranging from 20 to 30 W/m²K. While smaller bottles like Sting and Carolina show slight increases in HT, the effect is more pronounced in larger bottles as the air velocity increases.

The high air velocity exhibits the highest HT coefficients, with values between 30 and 40 W/m²K. Smaller bottles such as Sting and AXL show the most significant increases in HT, emphasizing the role of increased air velocity in boosting convective HT. However, larger bottles see a gradual decrease in HT as diameter increases.

The right axis, representing the average bottle diameter in mm, highlights that smaller-diameter bottles (Sting and Axl) benefit more from higher air velocities in terms of HT. In contrast, larger bottles (Carolina, Grip Tight) experience lower convective HT coefficients at both medium and high air velocities due to their larger surface area and reduced interaction with airflow. The chart thus underscores the combined influence of airflow velocity and bottle size on thermal performance in heating processes.

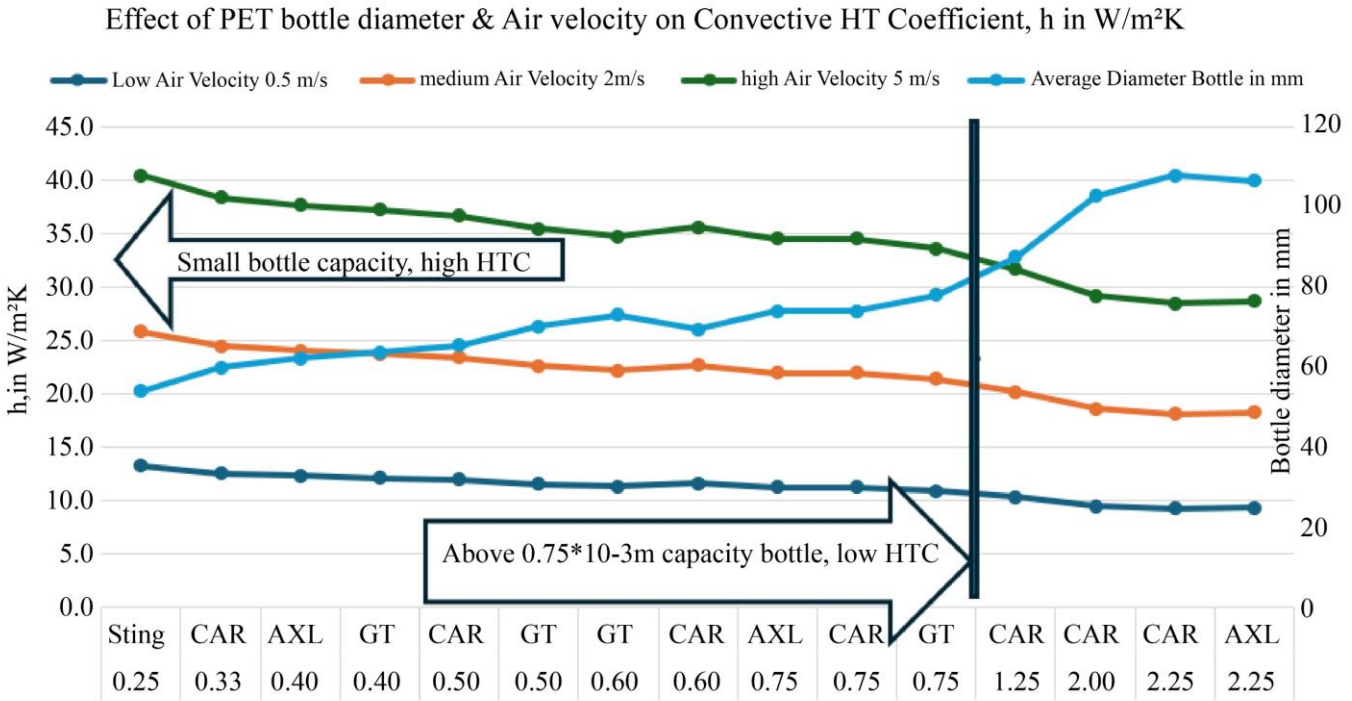

Fig. 8 The effect of PET bottle diameter and air velocity on the HT coefficient

5.1.2. Limitations of PET Bottles in Heat Removal Compared to Advanced Systems

The key limitation of using PET bottles with hot air for heat removal in the described system lies in their relatively low thermal conductivity compared to water spray-based. While hot air for PET bottles is a cost-effective and practical solution, their thermal efficiency is constrained by the inherent properties of PET material, which slows the heat transfer rate. This can result in less uniform temperature distribution, potentially affecting the consistency and quality of chilled beverages. Additionally, the reliance on convective heat transfer through airflow over bottle surfaces makes the system sensitive to airflow dynamics, which must be optimised.

5.1.3. Mitigation Strategies

To mitigate these limitations, bottle design enhancements, such as adding surface modifications with higher thermal conductivity, can be explored. Another effective strategy is optimizing airflow patterns using Computational Fluid Dynamics (CFD) simulations to ensure uniform distribution over bottle surfaces. Additionally, integrating hybrid systems where PET bottles work alongside more advanced thermal management systems—like liquid cooling advanced vibration system or dynamic motion of bottles—can improve overall efficiency while maintaining cost-effectiveness. These adjustments ensure better performance without relying on PCMs unsuitable for food-related applications.

6. Conclusion and Future Work

6.1. Discussion on Achieving Better Results Compared to State-of-the-Art Techniques

In this study, we observed that certain parameters—such as bottle size, arrangement, air velocity, and inlet temperature—directly affect the Heat Transfer (HT) performance in PET bottles placed in heating tunnels. Our findings demonstrate better thermal efficiency compared to existing methods reported in the literature, and the following key aspects explain why and how we achieved these improved results.

- Smaller Bottle Sizes and Higher Air Velocities: Previous studies have shown varying degrees of success in using bottle configurations to improve HT efficiency. However, many of these studies primarily focused on standard bottle sizes or configurations without fully exploiting the impact of smaller bottle sizes and airflow velocity. Our work found that smaller bottles, such as the 250 mL Sting bottles, demonstrated higher heat transfer rates, particularly at higher air velocities. This contrasts with some state-of-the-art studies that did not emphasize the impact of air velocity on smaller bottles or neglected the potential of high Reynolds and Nusselt numbers, which directly correlate with improved convective heat transfer. By focusing on optimizing both these parameters—bottle size and airflow—we were able to achieve superior heat transfer efficiency.
- Staggered vs. Inline Bottle Arrangement: One of the significant findings of our study was the superior performance of staggered bottle arrangements over inline configurations, which is often not a focal point in many previous studies. In state-of-the-art techniques, inline bottle arrangements are frequently used due to their simplicity in design. However, staggered arrangements result in improved heat transfer because they enhance air interaction with each bottle's surface, leading to better thermal efficiency. Our results, which align with flow dynamics principles, showed that staggered arrangements lead to higher convective heat transfer, particularly at higher Reynolds numbers. This finding significantly improved over previous approaches, where bottle arrangement was not given as much attention as factors like air velocity or surface material.
- Impact of Bottle Size on HT Coefficient: A key contribution of our study is the in-depth analysis of the effect of bottle size on the HT coefficient. As bottle size increases, the HT coefficient decreases due to a reduced surface area interacting with the airflow. Many prior studies have neglected this aspect or used a limited range of bottle sizes. By systematically analysing a wide range of bottle sizes, we demonstrated that smaller bottles yield better heat transfer characteristics. This factor has often been overlooked in previous works. The insights from this analysis can help optimize heating systems for beverage packaging, particularly when scaling production to larger bottles without sacrificing thermal efficiency.
- Comprehensive Optimization of Thermal Efficiency: Unlike earlier works that focused on a single parameter (e.g., air velocity or bottle arrangement) to improve HT efficiency, our study employed a comprehensive approach considering multiple interacting factors simultaneously. We achieved an optimised thermal performance by examining the combined effects of bottle size, arrangement, air velocity, and inlet temperature. This holistic approach contrasts with prior studies that often isolated these factors, resulting in incomplete optimization. Our work demonstrated higher efficiency and provided valuable insights into the specific combinations of these factors that result in improved heat transfer.
- Enhanced Efficiency with Solar Heating Systems: The theoretical focus of our work on employing PET bottles for thermal energy transfer via solar heating systems represents a novel and sustainable approach. While PET bottles have been used extensively in packaging, their potential in thermal systems, particularly in solar energy applications, has not been explored in-depth in the literature. By optimizing the heat transfer properties of PET bottles in thermal applications, our study paves the way for more energy-efficient and environmentally friendly heating systems, which aligns with global trends

towards sustainability in manufacturing processes. This approach offers better thermal efficiency and a reduction in energy consumption, contributing to the broader goal of minimizing environmental impact.

- The improved results achieved in this study are primarily due to the comprehensive and systematic investigation of key parameters, such as bottle size, arrangement, air velocity, and inlet temperature, that influence the heat transfer process in PET bottles placed in heating tunnels. Smaller bottles, such as the 0.250 x10-3 m3 Sting, exhibit higher HT rates than larger ones like the 2.250 x10-3 m3 Carolina, especially at higher air velocities. Staggered bottle configurations consistently outperform inline arrangements in terms of thermal efficiency. As the Reynolds and Nusselt numbers increase with airflow velocity, convective HT improves, particularly for staggered configurations. However, as bottle size increases, the HT coefficient decreases due to reduced surface area interaction with airflow. By employing a holistic optimization approach and focusing on factors that have been underexplored in previous studies, we significantly enhanced the heating process's thermal efficiency. These findings directly apply to optimizing heating systems in beverage packaging and suggest avenues for further research, especially in the context of solar heating systems and environmentally sustainable practices.

Abbreviation

Latent heat thermal energy storage systems = LHTESS
Virtual Power Plant = VPP
Heat Transfer = HT
Thermal energy storage = TES
Demand Response studies = DRS
Heat transfer fluid = HTF
Renewable Energy source= RES
Phase change materials = PCMs
Heat exchanger = HE
Sensible Heat System = SHS
Heat storage = HS
thermal conductivity = TC
Latent Heat Storage= LHS

References

[1] George Dogkas et al., "Development and Experimental Testing of a Compact Thermal Energy Storage Tank Using Paraffin Targeting Domestic Hot Water Production Needs," *Thermal Science and Engineering Progress*, vol. 19, pp. 1-9, 2020. [CrossRef] [Google Scholar] [Publisher Link]

[2] Francis Agyenim et al., "A Review of Materials, Heat Transfer and Phase Change Problem Formulation for Latent Heat Thermal Energy Storage Systems (LHTESS)," *Renewable and Sustainable Energy Reviews*, vol. 14, no. 2, pp. 615-628, 2010. [CrossRef] [Google Scholar] [Publisher Link]

[3] Loa Karjalainen, "Packaging of Carbonated Beverages," *Modern Processing, Packaging and Distribution Systems for Food*, Boston, MA: Springer US, pp. 110-131, 1987. [CrossRef] [Google Scholar] [Publisher Link]

[4] Jr. Carl R. Howard, "Blow Molded Container with Self-Supporting Base Reinforced By Hollow Ribs," *U.S. Patent 4850494A*, pp. 1-6, 1989. [Google Scholar] [Publisher Link]

[5] Dennis L. Marshall et al., "Plastic Container with Reinforcing Ring in the Base," *U.S. Patent 4955491A*, pp. 1-14, 1990. [Google Scholar] [Publisher Link]

[6] Vasiliki F. Alexiou et al., "Poly (Ethylene Terephthalate) Carbon-Based Nanocomposites: A Crystallization and Molecular Orientation Study," *Polymers*, vol. 12, no. 11, pp. 1-14, 2020. [CrossRef] [Google Scholar] [Publisher Link]

[7] Jianping Ma et al., "Structure–Property Evolution of Poly (Ethylene Terephthalate) Fibers in Industrialized Process Under Complex Coupling of Stress and Temperature Field," *Macromolecules*, vol. 52, no. 2, pp. 565-574, 2018. [CrossRef] [Google Scholar] [Publisher Link]

[8] Mélanie Girard, Christelle Combeaud, and Noëlle Billon, "Effects of Annealing Prior to Stretching on Strain Induced Crystallization of Polyethylene Terephthalate," *Polymer*, vol. 230, pp. 1-23, 2021. [CrossRef] [Google Scholar] [Publisher Link]

[9] D. Karalekas et al., "Numerical and Experimental Investigation of the Deformational Behaviour of Plastic Containers," *Packaging Technology and Science: An International Journal*, vol. 14, no. 5, pp. 185-191, 2001. [CrossRef] [Google Scholar] [Publisher Link]

[10] Kunlapat Thongkaew, and Thanwit Naemsai, "Mechanical Properties and Cost-Minimized Design of 6-Litre PET Bottle Using Finite Element Method," *Walailak Journal of Science and Technology*, vol. 17, no. 6, pp. 579-587, 2020. [CrossRef] [Google Scholar] [Publisher Link]

[11] D. Battini et al., "Experimental Characterisation and Modelling of Polyethylene Terephthalate Preform for Injection Stretch Blow Moulding," *International Journal of Materials and Product Technology*, vol. 60, no. 1, pp. 18-39, 2020. [CrossRef] [Google Scholar] [Publisher Link]

[12] Ibrahim Dincer, and Marc A. Rosen, *Thermal Energy Storage: Systems and Applications*, John Wiley & Sons, pp. 1-624, 2011. [Google Scholar] [Publisher Link]

[13] Huili Zhang et al., "Thermal Energy Storage: Recent Developments and Practical Aspects," *Progress in Energy and Combustion Science*, vol. 53, pp. 1-40, 2016. [CrossRef] [Google Scholar] [Publisher Link]

[14] A. Abhat, "Low Temperature Latent Heat Thermal Energy Storage: Heat Storage Materials," *Solar Energy*, vol. 30, no. 4, pp. 313-332, 1983. [CrossRef] [Google Scholar] [Publisher Link]

[15] Ingo Stadler, Andreas Hauer, and Thomas Bauer, "Thermal Energy Storage," *Handbook of Energy Storage: Demand, Technologies, Integration*, pp. 563-609, 2019. [CrossRef] [Google Scholar] [Publisher Link]

[16] R. Parameshwaran, and Siva Kalaiselvam, "Nanomaterial-Based PCM Composites for Thermal Energy Storage in Buildings," *Nano and Biotech Based Materials for Energy Building Efficiency*, pp. 215-243, 2016. [CrossRef] [Google Scholar] [Publisher Link]

[17] Huangjie Gong et al., "Demand Response of HVACs in Large Residential Communities Based on Experimental Developments," *IEEE Energy Conversion Congress and Exposition*, Detroit, MI, USA, pp. 4545-4548, 2020. [CrossRef] [Google Scholar] [Publisher Link]

[18] Dogan Erdemir et al., "Energy Storage Techniques for Renewables," *Renewable Energy Based Solutions,* Cham: Springer International Publishing, pp. 425-450, 2022. [CrossRef] [Google Scholar] [Publisher Link]

[19] Sandris Rucevskis, Pavel Akishin, and Aleksandrs Korjakins, "Performance Evaluation of an Active PCM Thermal Energy Storage System for Space Cooling in Residential Buildings," *Environmental and Climate Technologies*, vol. 23, no. 2, pp. 74-89, 2019. [CrossRef] [Google Scholar] [Publisher Link]

[20] Dogan Erdemir, "Determination of Effect of Bottle Arrangement in the Sensible Thermal Energy Storage System Consisting of Water-Filled PET Bottles on Thermal Performance," *Hittite Journal of Science and Engineering*, vol. 6, no. 4, pp. 235-242, 2019. [CrossRef] [Google Scholar] [Publisher Link]

[21] Zhen Qin et al., "Geometry Effect of Phase Change Material Container on Waste Heat Recovery Enhancement," *Applied Energy*, vol. 327, 2022. [CrossRef] [Google Scholar] [Publisher Link]

[22] Mohamed E.A.E. Ahmed et al., "Finned-Encapsulated PCM Pyramid Solar Still–Experimental Study with Economic Analysis," *Journal of Energy Storage*, vol. 73, 2023. [CrossRef] [Google Scholar] [Publisher Link]

[23] Dogan Erdemir, and Necdet Altuntop, "Thermodynamic Analysis of Sensible Thermal Energy Storage in Water Filled PET Bottles," *International Journal of Exergy*, vol. 26, no. 1-2, pp. 77-92, 2018. [CrossRef] [Google Scholar] [Publisher Link]

[24] Flavio Roberto Ceja Soto et al., "Sustainability Metrics for Housing and the Thermal Performance Evaluation of a Low-Cost Prototype Made with Poly (Ethylene Terephthalate) Bottles," *Recycling*, vol. 4, no. 3, pp. 1-16, 2019. [CrossRef] [Google Scholar] [Publisher Link]

[25] K.S. Reddy, Vijay Mudgal, and T.K. Mallick, "Review of Latent Heat Thermal Energy Storage for Improved Material Stability and Effective Load Management," *Journal of Energy Storage,* vol. 15, pp. 205-227, 2018. [CrossRef] [Google Scholar] [Publisher Link]

[26] K.A.R. Ismail, and J.R. Henríquez, "Thermally Effective Windows with Moving Phase Change Material Curtains," *Applied Thermal Engineering*, vol. 21, no. 18, pp. 1909-1923, 2001. [CrossRef] [Google Scholar] [Publisher Link]

[27] Ioannis Sifnaios et al., "Evaluation of Stratification in Thermal Energy Storages," *Renewable Energy Systems in Smart Grid*, pp. 57-69, 2022. [CrossRef] [Google Scholar] [Publisher Link]

[28] Fatih Selimefendigil, and Hakan F. Öztop, "Analysis of Hybrid Nanofluid and Surface Corrugation in the Laminar Convective Flow through an Encapsulated PCM Filled Vertical Cylinder and POD-Based Modeling," *International Journal of Heat and Mass Transfer*, vol. 178, 2021. [CrossRef] [Google Scholar] [Publisher Link]

[29] Mahmoud Moeini Sedeh, and J.M. Khodadadi, "Thermal Conductivity Improvement of Phase Change Materials/Graphite Foam Composites," *Carbon*, vol. 60, pp. 117-128, 2013. [CrossRef] [Google Scholar] [Publisher Link]

[30] Zhongbin Zhang, Meng Liang, and Zhongqiu Ci, "Thermal Performance Analysis of Latent Heat Thermal Energy Storage with Cascaded Phase Change Materials Capsules Under Varying Inlet Temperature," *Journal of Energy Storage*, vol. 62, 2023. [CrossRef] [Google Scholar] [Publisher Link]

[31] Ashmore Mawire, Katlego A. Lentswe, and Adedamola Shobo, "Performance Comparison of Four Spherically Encapsulated Phase Change Materials for Medium Temperature Domestic Applications," *Journal of Energy Storage*, vol. 23, pp. 469-479, 2019. [CrossRef] [Google Scholar] [Publisher Link]

[32] Atul Sharma et al., "Review on Thermal Energy Storage with Phase Change Materials and Applications," *Renewable and Sustainable Energy Reviews*, vol. 13, no. 2, pp. 318-345, 2009. [CrossRef] [Google Scholar] [Publisher Link]

[33] Ioan Sarbu, and Calin Sebarchievici, "A Comprehensive Review of Thermal Energy Storage," *Sustainability*, vol. 10, no. 1, pp. 1-32, 2018. [CrossRef] [Google Scholar] [Publisher Link]

[34] Charalambos N. Elias, and Vassilis N. Stathopoulos, "A Comprehensive Review of Recent Advances in Materials Aspects of Phase Change Materials in Thermal Energy Storage," *Energy Procedia*, vol. 161, pp. 385-394, 2019. [CrossRef] [Google Scholar] [Publisher Link]

[35] Wen-Ya Wu et al., "Advancements in Sustainable Phase Change Materials: Valorizing Waste for Eco-Friendly Applications," *Materials Today Chemistry*, vol. 39, 2024. [CrossRef] [Google Scholar] [Publisher Link]

[36] Ana M. López-Sabirón et al., "Environmental Profile of Latent Energy Storage Materials Applied to Industrial Systems," *Science of the Total Environment*, vol. 473-474, pp. 565-575, 2014. [CrossRef] [Google Scholar] [Publisher Link]

[37] R. Bharathiraja et al., "Performance Investigation on Flat Plate Solar Water Collector Using a Hybrid Nano-Enhanced Phase Change Material (PCM)," *Journal of Energy Storage*, vol. 86, no. A, 2024. [CrossRef] [Google Scholar] [Publisher Link]

[38] Robert Hoel Lund, "*Optimized and Cost Efficient Industrial Heat Pumps based on Low Grade Waste Heat*," Master's Thesis, 2016. [Google Scholar] [Publisher Link]

[39] Pablo Dolado et al., *PCM-Air Heat Exchangers: Slab Geometry*, Heat Exchangers-Basics Design Applications, 2012. [Google Scholar] [Publisher Link]

[40] Pramod B. Salunkhe, and Jaya Krishna Devanuri, "Containers for Thermal Energy Storage," *Micro-and Nano-Containers for Smart Applications,* Singapore: Springer Nature Singapore, pp. 289-307, 2022. [CrossRef] [Google Scholar] [Publisher Link]

[41] Mohammed M. Farid et al., "A Review on Phase Change Energy Storage: Materials and Applications," *Energy Conversion and Management*, vol. 45, pp. 9-10, pp. 1597-1615, 2004. [CrossRef] [Google Scholar] [Publisher Link]

[42] Shobhana Singh et al., "Investigation on Transient Performance of a Large-Scale Packed-Bed Thermal Energy Storage," *Applied Energy*, vol. 239, pp. 1114-1129, 2019. [CrossRef] [Google Scholar] [Publisher Link]

[43] Pramod B. Salunkhe, and Prashant S. Shembekar, "A Review on Effect of Phase Change Material Encapsulation on the Thermal Performance of a System," *Renewable and Sustainable Energy Reviews*, vol. 16, no. 8, pp. 5603-5616, 2012. [CrossRef] [Google Scholar] [Publisher Link]

[44] Vennapusa Jagadeeswara Reddy et al., "Pathway to Sustainability: An Overview of Renewable Energy Integration in Building Systems," *Sustainability*, vol. 16, no. 2, pp. 1-36, 2014. [CrossRef] [Google Scholar] [Publisher Link]

[45] E.D. Grimison, "Correlation and Utilization of New Data on Flow Resistance and Heat Transfer for Cross Flow of Gases over Tube Banks," *Transactions of the American Society of Mechanical Engineers*, vol. 59, no. 7, pp. 583-594, 1937. [CrossRef] [Google Scholar] [Publisher Link]

[46] J.P. Holman, *Heat Transfer,* McGraw-Hill, Newyork, 2014. [Publisher Link]

[47] William S. Janna, *Engineering Heat Transfer,* CRC Press, 2018. [CrossRef] [Google Scholar] [Publisher Link]